

Folding concave polygons into convex polyhedra: The L-Shape

Emily Dinan
University of Washington

Alice Nadeau
University of Minnesota

Isaac Odegard
University of North Dakota

Follow this and additional works at: <https://scholar.rose-hulman.edu/rhumj>

Recommended Citation

Dinan, Emily; Nadeau, Alice; and Odegard, Isaac (2015) "Folding concave polygons into convex polyhedra: The L-Shape," *Rose-Hulman Undergraduate Mathematics Journal*: Vol. 16 : Iss. 1 , Article 13.
Available at: <https://scholar.rose-hulman.edu/rhumj/vol16/iss1/13>

ROSE-
HULMAN
UNDERGRADUATE
MATHEMATICS
JOURNAL

FOLDING CONCAVE POLYGONS INTO CONVEX POLYHEDRA: THE L-SHAPE

Emily Dinan^a Alice Nadeau^b Isaac Odegard^c

VOLUME 16, No. 1, SPRING 2015

Sponsored by

Rose-Hulman Institute of Technology

Department of Mathematics

Terre Haute, IN 47803

Email: mathjournal@rose-hulman.edu

<http://www.rose-hulman.edu/mathjournal>

^aUniversity of Washington

^bUniversity of Minnesota

^cUniversity of North Dakota

ROSE-HULMAN UNDERGRADUATE MATHEMATICS JOURNAL

VOLUME 16, NO. 1, SPRING 2015

FOLDING CONCAVE POLYGONS INTO CONVEX POLYHEDRA: THE L-SHAPE

Emily Dinan

Alice Nadeau

Issac Odegard

Abstract. Mathematicians have long been asking the question: Can a given convex polyhedron be unfolded into a polygon and then refolded into any other convex polyhedron? One facet of this question investigates the space of polyhedra that can be realized from folding a given polygon. While convex polygons are relatively well understood, there are still many open questions regarding the foldings of non-convex polygons. We analyze these folded realizations and their volumes derived from the polygonal family of ‘L-shapes,’ parallelograms with another parallelogram removed from a corner. We investigate questions of maximal volume, diagonal flipping, and topological connectedness and discuss the family of polyhedra that share a L-shape polygonal net.

Acknowledgements: We gratefully acknowledge support from NSF grant DMS-1063070 and the 2012 Lafayette College Research Experience for Undergraduates, where the majority of this research was undertaken. We would like to thank our research advisor, Dr. Kevin Hartshorn, who helped us with his great ideas, feedback, problem solving abilities and support throughout the project. We would especially like to thank Dr. Lu and Dr. Berkove, both at Lafayette College, for their continued support throughout the paper-writing process.

1 Introduction

Questions of folding and unfolding polyhedra have intrigued mathematicians since the days of Albrecht Dürer, the famed German Renaissance printmaker. His 1525 work, *Painter's Manual*, contains some of the earliest known examples of a polyhedral nets, or unfolded polyhedra made to lie flat for the purpose of printing. Since that time, great strides have been made toward understanding the relationship between polyhedra and polygons. In 2012, Erik Demaine, Martin Demaine, Jin-ichi Itoh, Anna Lubiw, Chie Nara, and Joseph O'Rourke demonstrated that every convex polyhedron may be unfolded to one planar piece and then refolded to some different convex polyhedron [6]. The question remains: can a given convex polyhedron be unfolded and then refolded (a finite number of times) into *any* other convex polyhedra? And if not, what are the equivalence classes in this space of polyhedra?

This paper endeavors to explore one aspect of this question with the aim toward a better understanding of equivalence relations in polyhedral space. We study the family of the “L-shapes”—parallelograms with another cut out of one corner—as polyhedral nets. We enumerate all of the possible gluings of these shapes using an algorithm developed (independently) by Anna Lubiw and Koichi Hirata [9]. We then employ our own algorithms to create the three-dimensional realizations of these gluings using the computer algebra system *Mathematica*. We discuss the family of polyhedra that can be related via this family of L-shapes as well as the topological properties of this spectrum.

In 2006, Demaine and O'Rourke posed the question, “Along all planar convex shapes of unit area (smooth shapes or polygons), which folds, via perimeter halving, to the maximum volume (convex) 3D shape?” [8]. This question must be adapted to deal with non-convex polygons, as the process of perimeter halving is not guaranteed to yield a convex polyhedron. We explore the maximal volumes that can be achieved through each combinatorial folding, each particular polygon, and finally, the entire family of L-shapes.

Over the course of our analysis, several challenges arose which are interesting in their own right. We discuss these phenomena diagonal flipping and edge relocation in detail in our paper. Both topics are important to understand in order to develop fast and accurate algorithms that generate three dimensional realizations of gluings.

In Section 2 we give an overview of relevant definitions and background material integral for understanding the results of this paper. We begin Section 3 by enumerating edge-to-edge gluing results for the right angled L-shape and discussing results due to changing this angle. This leads nicely to Section 4 where we prove that the topology of the space of foldings of general L-shapes (convex three-dimensional polyhedra can be generated from a particular L-shape by deforming the gluing of its boundary) is six isolated polytopes and five connected components. In Section 5 we briefly discuss the phenomenon of diagonal flipping which is important in the context of creating the three-dimensional realization of a folding. In Section 6 we discuss what happens to a crease pattern as a polygon approaches a flat folding and prove that exactly one edge relocates in the crease pattern after the flat folding. In Section 7 we discuss how different foldings of the same polygon affect the volume enclosed by the three-dimensional realization. Finally, in Section 8 we pose questions for future work.

2 Background and Definitions

Here we briefly discuss prior results regarding the folding of the square and the rectangle and related terms, definitions and notations. Henceforth, these terms will be used freely. Readers familiar with polygon folding should feel free to skip to the last paragraph in this section where we briefly discuss the definition of an L-shape.

Recent work in folding and unfolding polyhedra relies heavily on the work of Aleksandr Alexandrov. Specifically, Alexandrov's Theorem [8] has been the backbone for much of the work in polyhedra:

Theorem 1 (Alexandrov's Theorem) *Any such gluing of polygons that*

1. *uses up the perimeter of all the polygons with boundary matches;*
2. *glues no more than 2π total angle of the polygon material at any point; and*
3. *results in a complex homeomorphic to a sphere,*

corresponds to a unique convex polyhedron.

Alexandrov proved this theorem in 1942, but its connection with folding polyhedra was not made until much later by Anna Lubiw and Joseph O'Rourke in 1996. They used Alexandrov's Theorem to implement their dynamic programming algorithm for finding convex polyhedra realized from folding polygons [9].

Here we give an example of a folding that satisfies the conditions of Alexandrov's Theorem (and, thus, corresponds to a unique convex polyhedron). The image in Figure 1 illustrates the folding of a Latin Cross into a cube. This folding satisfies Alexandrov's theorem. First, the entire perimeter of the Latin Cross is glued, as can be seen in the picture. Second, no more than 2π total angle is glued at any point. For instance, at each corner of the resulting cube $\frac{3}{2}\pi$ angle of the polygonal material is being glued together and all other places there is 2π of polygonal material. Lastly, the resulting hexahedron is clearly homeomorphic to a sphere.

In 2000, Erik Demaine, Martin Demaine, Anna Lubiw, and Joseph O'Rourke briefly discussed folding a rectangle in their work *Examples, Counterexamples, and Enumeration Results for Foldings and Unfoldings between Polygons and Polytopes* [7]. They show that any rectangle may fold to an uncountable number of distinct tetrahedra [7]. This proof relies on analyzing the *gluing tree*, T_G , of a particular gluing G , where T_G is a double-edged labeled "tree" representing the combinatorial structure of G [8] (for a detailed description of a gluing tree see the next paragraph and Figure 2). A *node* on a gluing tree is the part of the gluing in which a vertex from the polygon is glued to some other part of the polygon. Note that a polygonal vertex may be glued to a polygonal edge, a polygonal vertex, or any combination of the two so long as it satisfies Alexandrov's Theorem. The *leaves* of T_G may be either convex-vertex leaves or fold points. A *convex-vertex leaf* is a leaf where the edges on opposite sides of the vertex are glued together leaving the vertex at the tip of the leaf, and a *fold point* is a leaf where an edge is glued to itself.

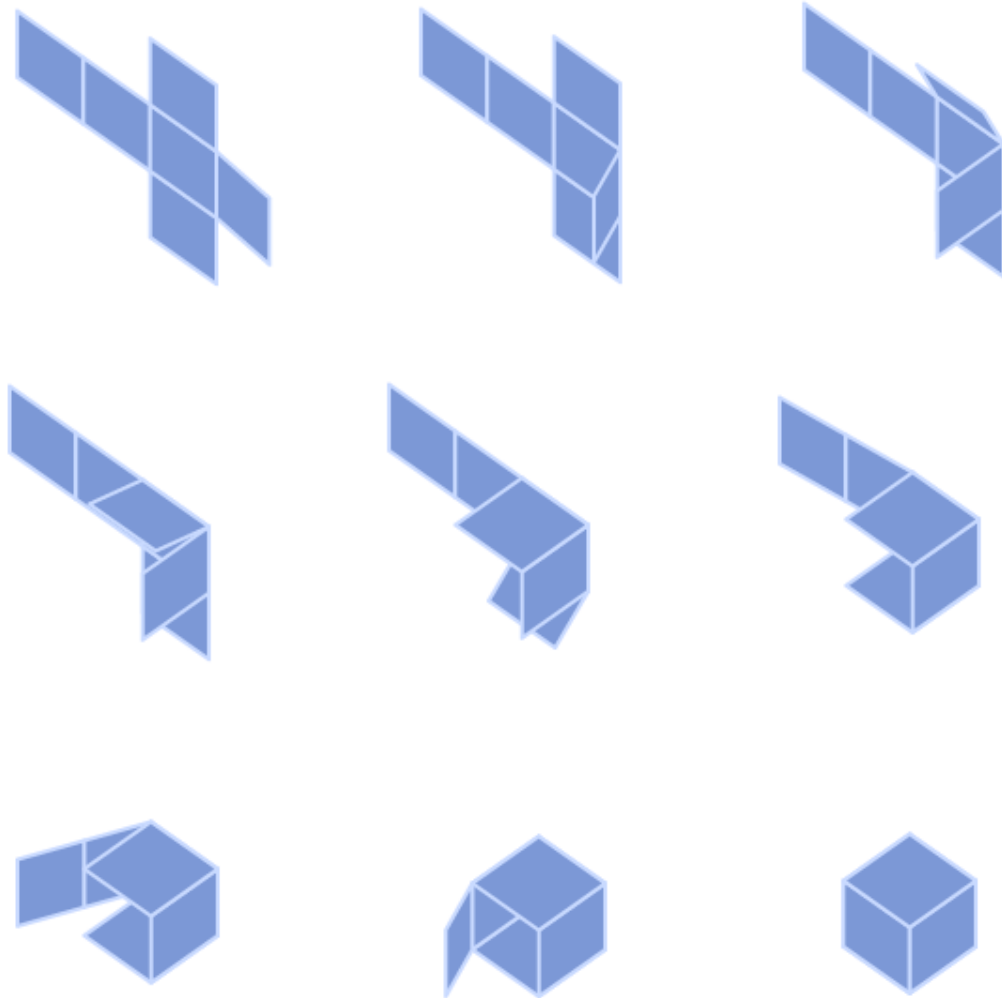


Figure 1: Snapshots of the folding of the Latin Cross into a cube. We see the flat polygon slowly deform into the 3D polyhedron going left to right from the upper left and ending at the lower right. Note, the first image is shown in perspective (the Latin Cross is actually six squares).

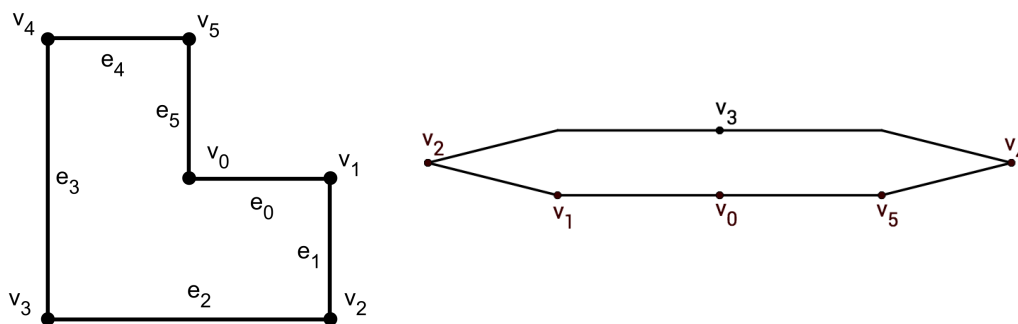


Figure 2: An L-shape with edges and vertices labeled (*left*) and a gluing tree for the L-shape (*right*). The tree shows how vertices and edges are glued together.

Figure 2 gives us an example of a gluing tree. In this example, we see that the tree had three nodes: the first is where vertex v_3 and vertex v_0 are glued together (indicated by vertex v_3 being placed directly above v_0 in Figure 2), the second where vertex v_1 is glued to edge e_2 (indicated by the kink in the edge above v_1), and the third where vertex v_5 is glued to edge e_3 (indicated by the kink in the edge above v_5). This tree has two leaves, both of which are convex vertex leaves. The convex-vertex leaves are represented by the points at vertices v_2 and v_4 on the gluing tree, indicating that the edges adjacent to these polygonal vertices must be glued together. There are no leaves that are fold points for this gluing tree, but if there were they would have rounded edges as in Figure 5.

The proof that the rectangle produces an infinite number of distinct tetrahedra relies on the concept of the rolling belt. A *rolling belt* is a path in a gluing tree that: (1) connects two leaves (either convex-vertex or fold-point leaves) and (2) has face angle of $\leq \pi$ along the entire path [8]. It is called a rolling belt because when we connect the two leaves, we can halve the perimeter and glue along any point, or “roll the belt.” This results in an infinite number of gluings. See Figure 5 for an example of a gluing tree with a rolling belt. The vertical loop along the left hand side of the gluing tree indicates that a rolling belt exists where vertices 3 and 4 are glued together. Note that π angle of polygonal material is glued together at this connection of two leaves, satisfying the conditions of a rolling belt. We can “halve” the resulting loop at any point along the leftmost edge of the shape.

Not all gluing trees have rolling belts. The gluing tree in Figure 2 has no rolling belts, for instance. At every point where two leaves are connected, more than π angle of polygonal material is glued together, violating the conditions for a rolling belt. (For instance, vertex 3 and vertex 0 are glued together, resulting in 2π angle of material being glued together.) Hence, this gluing tree does *not* yield an infinite variety of polyhedral realizations. In the case of the polygonal Latin Cross, previously studied by Rebecca Alexander, Heather Dyson, Martin Demaine, Anna Lubiw, and Koichi Hirata, there are *no* rolling belts in any of the gluing trees [8]. The 85 combinatorially distinct foldings of this shape (only 23 of which are geometrically distinct) form a discrete topology. The work on the Latin Cross inspired our

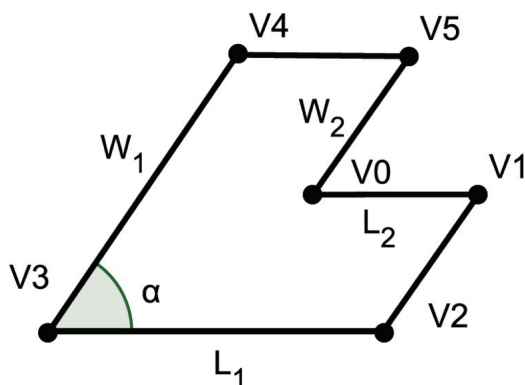


Figure 3: The general L-shape. $W_2 = 0$ or $L_2 = 0$ yields a parallelogram.

work on other non-convex polygons, specifically the family of L-shapes.

In 2002, Rebecca Alexander, Heather Dyson, and Joseph O'Rourke studied in depth the foldings of the square to convex polyhedra. They discovered that five families of polyhedra (tetrahedra, two different pentahedra, hexahedra, and octahedra) and four combinatorially distinct flat polyhedra (a triangle, square, rectangle, and pentagon) were realizable from folding the square. They were able to illustrate that these families of polyhedra are continuously deformable into each other via a sequence of rolling belts [4]. They also showed that the polyhedron of largest volume realized from the square was an octahedron obtained via *perimeter halving*. Given two antipodal points x, y on the boundary of a polygon where $P(x, y)$ is the open interval counterclockwise from x to y , *perimeter halving* is a method of gluing that identifies $P(x, y)$ to $P(y, x)$ [8].

The two other methods for folding a polygon are edge-to-edge gluings and general gluings. An *edge-to-edge gluing* is a method that requires whole edges be glued to whole edges. Edge-to-edge gluings may or may not be perimeter halvings and vice versa. The term *general gluing* encompasses all types of gluing (including perimeter halving and edge-to-edge gluings) with the requirement that the gluing satisfies Alexandrov's theorem [8]. Any gluing we refer to in this paper will satisfy Alexandrov's Theorem unless explicitly stated otherwise.

The efforts of these mathematicians are part of the larger goal of understanding the space of polyhedra realizable from the folding of any given polygon. We endeavor to continue this project by studying non-convex shapes, in particular L-shapes. An *L-shape* is a $L_1 \times W_1$ parallelogram with acute angle α and a $L_2 \times W_2$ parallelogram (where $L_2 < L_1$ and $W_2 < W_1$) cut out of one of the acute angled corners. In this paper, we enumerate the vertices of the L-shape clockwise as in Figure 3 and focus on the case in which $L_2 = \frac{1}{2}L_1$ and $W_2 = \frac{1}{2}W_1$. We refer to L-shapes of this form as *regular L-shapes*. Additionally, we assume all polygons have unit area.

3 Foldings of L-shapes

The foldings of convex polygons is, in general, well understood. In O'Rourke and Demaine's book on *Geometric Folding Algorithms*, they are able to list all possible combinatorial types of gluing trees for convex polygons of n -vertices [8]. Further, we know that any polyhedron folded from a convex n -gon has at most $n + 2$ vertices. The foldings of *regular* convex n -gons are described in even greater detail in their book. On the other hand, comparatively little work has been done in the area of non-convex polygons. This is perhaps due to the fact that, unlike convex polygons, not all non-convex polygons fold to polyhedra [7] because of part (2) of Alexandrov's Theorem. In order to get a grasp on non-convex polygons, we study the general "L-shape" beginning with the right angled L-shape.

3.1 The Right Angled L-Shape

The term "*right angled L-shape*" refers to the L-shape where $\alpha = \frac{\pi}{2}$ and $L_1 = \ell = 2L_2, W_i = L_i$. See Figure 2 or Figure 8 for a pictorial representation of the shape.

Implementing Lubiw's algorithm for enumerating the edge-to-edge foldings of a polygon [9], we discovered the 7 edge-to-edge foldings of the right angled L-shape where the edge of length 2 is taken as two edges of length 1 (as Demaine does in [8]). Only three of these foldings are geometrically distinct. Six out of seven are flat. We provide images in Figure 4.

Encompassing these 7 edge-to-edge gluings are the 49 combinatorially distinct general gluings. We used an algorithm based on Hirata's to enumerate these gluings [1]. Among these 49 gluings, 21 are redundant due to symmetry in the structure of the right angled L-shape. Due to the presence of rolling belts in several of the gluing structures, there are infinitely many geometrically distinct realizable polyhedra from this finite number of distinct combinatorial types.

While we may use an algorithm to determine the possible ways in which the edges of a given polygon may be glued to form a convex polyhedron, determining the edges along which to fold the polygon to realize the polyhedron remains difficult. Our current methods for performing this task are limited to physically folding a piece of paper, unfolding, and analyzing the crease pattern. One method used by other authors, including Alexander, Dyson, and O'Rourke, involves checking all possibilities [4]. In this vein, we hope to eventually produce an algorithm that will check every possible combination of edges between vertices, check for convexity, and determine the correct set of edge lengths for a particular folding. Until then, an example of our methods for completing this step are pictured in Figure 5. To find the edges of the polyhedron we parameterized the distance from vertex v_3 to the nearest fold point and then used the distance formula and crease pattern to determine the parameterized equations for edge length.

In 2008, Bobenko and Izvestiev presented a constructive proof of Alexandrov's theorem that would allow us to determine the resulting convex polytope with a given metric on the boundary [5]. In 2010, O'Rourke suggested that a more interesting direction for future research would be to explore classes of polyhedra reconstructable from an Alexandrov

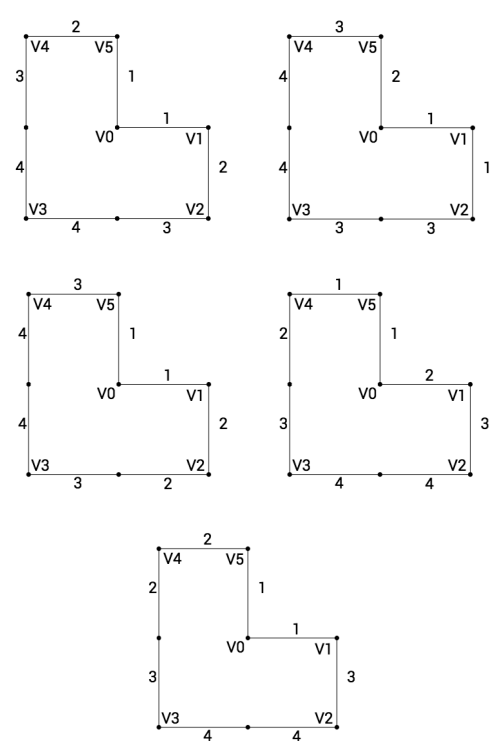
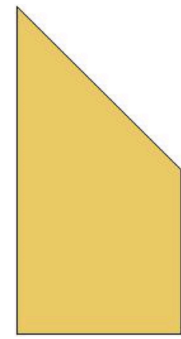
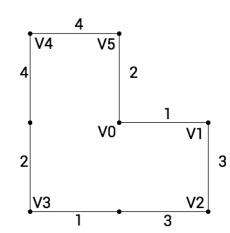

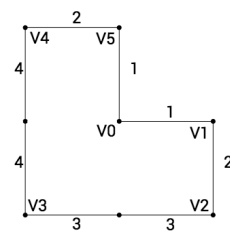
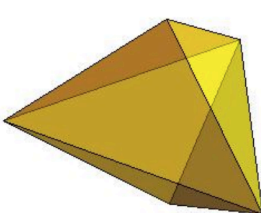
Gluing	3D Realization
 <p>The first row of the 'Gluing' column contains three diagrams. Each diagram shows a right-angled L-shape with vertices labeled V0 through V5. Numbers on the edges indicate which edges are to be glued together. The first diagram shows edges (V4,V5), (V0,V1), (V3,V2), and (V3,V4) being glued. The second diagram shows edges (V4,V5), (V0,V1), (V3,V2), and (V3,V4) being glued. The third diagram shows edges (V4,V5), (V0,V1), (V3,V2), and (V3,V4) being glued.</p>	 <p>A flat 3D realization of the L-shape, appearing as a yellow trapezoid.</p>
 <p>A diagram showing a different way to glue the edges of the L-shape. The numbers on the edges indicate which edges are to be glued together.</p>	 <p>A flat 3D realization of the L-shape, appearing as a yellow trapezoid.</p>
 <p>A diagram showing a different way to glue the edges of the L-shape. The numbers on the edges indicate which edges are to be glued together.</p>	 <p>A 3D realization of the L-shape, appearing as a yellow pyramid.</p>

Figure 4: The three distinct 3D realizations for all of the edge-to-edge foldings of the right angled L-Shape. In the “Gluing” column, numbers on edges represent which edges are glued together. In the “3D Realization” column we have the three geometrically distinct realizations of which the first two are flat.

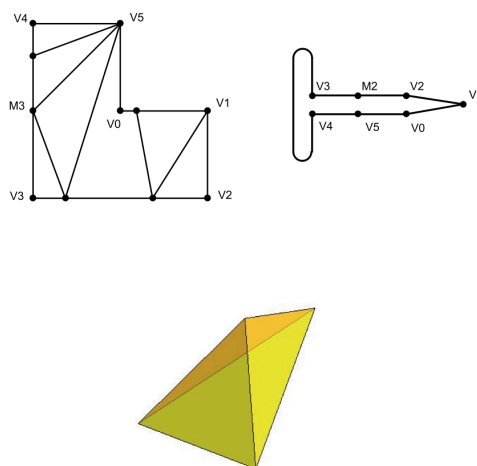


Figure 5: Simple folding example. Clockwise from top left: (i) Unglued L-shape with crease pattern (creases indicate where edges of the tetrahedron lie); (ii) Gluing tree showing which vertices/edges are glued together; (iii) 3D realization of the structure glued from (i).

gluing without all this machinery [10]. We take O'Rourke's comments as motivation for our work and developed algorithms in *Mathematica* to produce the three dimensional realizations for this family of L-shapes using the parameterized edge lengths. Again, despite the fact that there are a finite number of combinatorially distinct gluings, we have an infinite family of geometrically distinct realizations due to the presence of rolling belts in several of the gluing structures. The resulting structures include flat shapes, tetrahedra, hexahedra, degenerate pentahedra, octahedra, and degenerate heptahedra.

3.2 Varying the Angle

Several of the combinatorial structures that were achievable via folding the right angled L-shape are not valid when the angle α (see Figure 3) is varied on the interval $[0, \frac{\pi}{2}]$; when α becomes acute, certain gluing patterns yield non-convex polyhedra. For example, the gluing tree depicted by ring *A* in Figure 7, which yields a family of tetrahedra and a degenerate flat quadrilateral for the right angled L-shape, gives rise to non-convex polytopes when α is acute. This is the result of gluing an either obtuse vertices ($V2$ and $V4$ both have angle $\pi + \alpha$) into the reflex vertex ($V0$ has angle $2\pi - \alpha$), which is a clear violation of part (2) of Alexandrov's theorem.

Another interesting result is the appearance of a decahedron among the set of polyhedra realizable from this family of L-shapes. Unfortunately, the numerous diagonal flips in this figure, along with the increasing number of flips in the hexahedra and octahedra as α decreases, makes determining the convex three dimensional structure progressively more difficult.

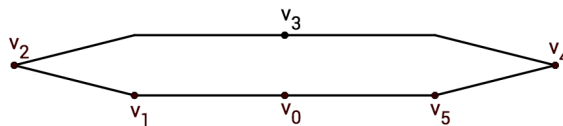


Figure 6: A gluing Tree for for an L-shape. This particular gluing has no rolling belt.

4 Topology of the Space of the Foldings of L-Shapes

Unlike the connected space of the foldings of the square [4], the space of the L-shape foldings is topologically *disconnected*. In Figure 7 we see a graphical representation of the particular topology of the foldings of the right angled L-shape. In the following section we show that the topology of any L-shape with $\alpha \leq \pi$ is disconnected then we prove that Figure 7 is the topology of the right L-shape.

Lemma 2 *For any non-convex L-shape, the topological space is disconnected.*

Proof: Using the labels provided in Figure 3, we may glue vertex $V3$ to vertex $V0$, and subsequently, half of L_1 to L_2 , half of W_1 to W_2 , and so on (as represented in Figure 6). Notice that this gluing is a perimeter halving, so we will satisfy Alexandrov's Theorem as long as no more than 2π total angle is glued at any point. We see that the only place of concern is the reflex vertex, $V0$. Note that there is no issue since we glue $V3$ to $V0$ resulting in exactly 2π total angle at that point. Furthermore, notice that the reflex vertex cannot be part of any rolling belt. As α is acute and the reflex angle sums to $2\pi - \alpha$, the conditions for a rolling belt (which require no more than π angle along the span of the belt) are clearly violated. Indeed, no part of the flying can be part of a rolling belt.

By symmetry, we consider only the righthand part of Figure 6. We see that the part of the flying to the right of the $V0V3$ glue point cannot be a rolling belt because we cannot glue any other vertex or edge at this point as it would violate part (2) of Alexandrov's Theorem. This forces us to glue the edge between $V0$ and $V5$ to the edge between $V3$ and $V4$ starting at $V3$. Now we glue until we get to $V5$, so it is natural to ask if the part of the gluing to the right of $V5$ is a rolling belt. Again, we see this is not the case because the point where $V5$ is glued to the edge $e3$ has $\pi + \alpha$ total angle, i.e. we can't glue an edge to this point, making a rolling belt impossible. Thus, this particular gluing may not be continuously deformed into any other and the space of the foldings of the L-shapes is topologically disconnected. ■

We now turn our attention to the topology of a particular L-shape, the right L-shape. In Figure 7 we chose to omit redundant gluing structures that exist as a result of the symmetry

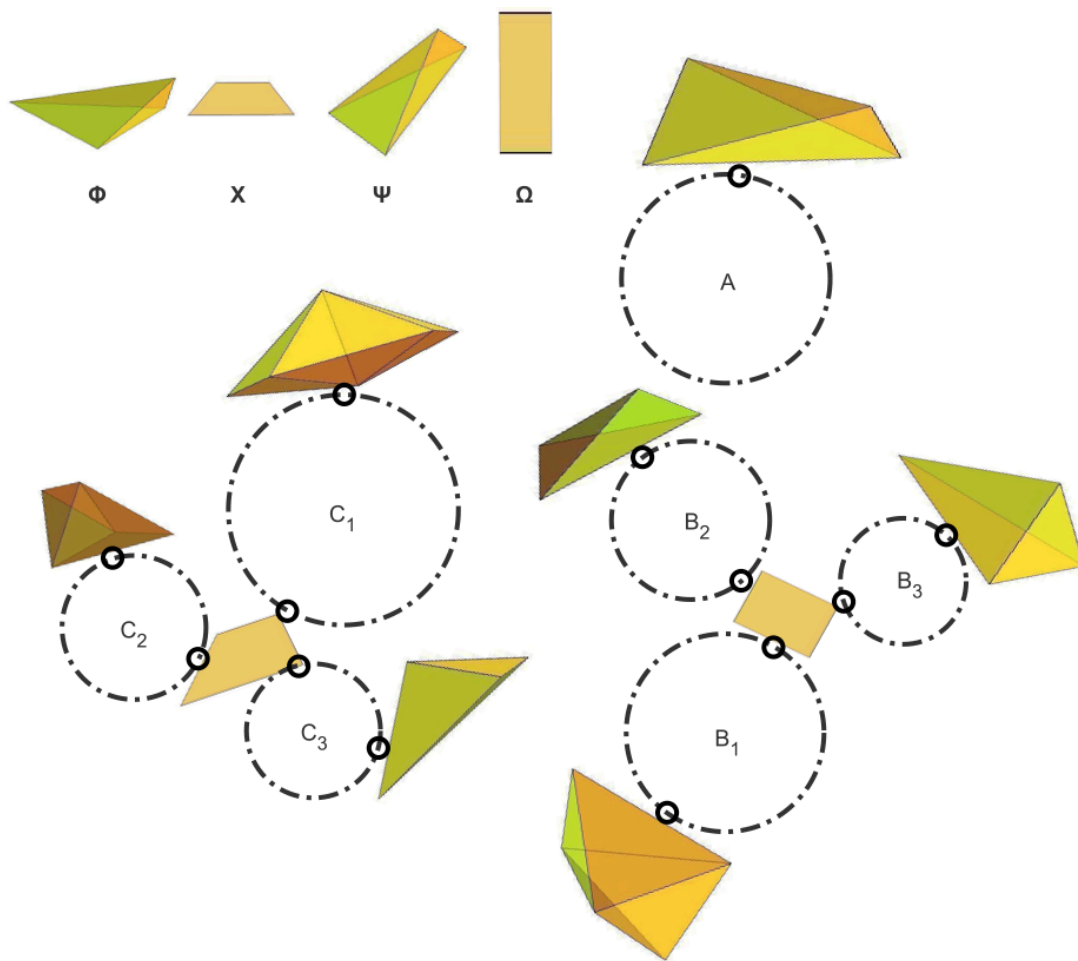


Figure 7: The topology of the space of the foldings of the right angled L-Shape. Dashed circles represent rolling belts on which infinitely many distinct polyhedron can be realized. Some polyhedra are shown here for reference.

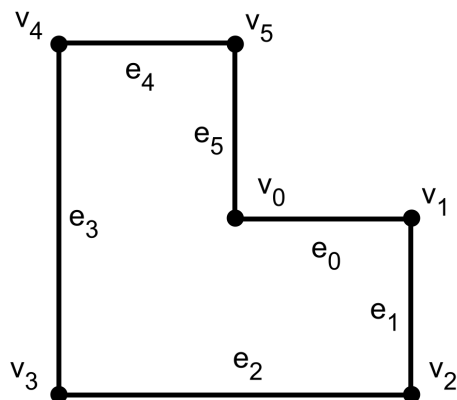


Figure 8: Edge and vertex labels for the right L-shape.

of the L-shape. We thus left out a copy of the isolated tetrahedron, rings A and B, and symmetric components of ring C. Including these redundancies, there are eleven separate components to the topology. We prove this in Theorem 2.

We will see that even though the L-shape is a non-convex polygon, it still has several rolling belts. The rolling belts are represented in Figure 7 by dashed rings. Though we only chose to represent one polyhedron per rolling belt, infinitely many geometrically distinct polyhedra are realized along each belt. The B and C rings are connected via flat foldings depicted in the diagram. Beyond this, though, there are no connections between the separate rolling belts as we will show in the proof. In other words, polyhedra from different rolling belts cannot be continuously deformed into each other, except in the case of the B and C rings.

Theorem 3 *The topological space of the foldings of the right-angled L-shape is six isolated shapes and five separate connected components.*

Proof: Throughout the proof, we will use the edge and vertex notation as depicted in Figure 8. Also note that in Figure 7 we see only three connected components. This is because, due to the symmetry of the right-angled L-shape, the B and C components each have an identical copy. These redundant components are mentioned in the proof but not proved because they follow directly by simply by changing the names of vertices already given.

We begin our investigations by separating cases based on which vertex may be glued into the reflex vertex, v_0 . Recall that no edge may be glued into the reflex vertex as this would violate part (2) of Alexandrov's Theorem. Due to the symmetry of the right angled L-shape, some cases are the same. The the four non-redundant cases are as follows:

1. Glue v_1 or v_5 to v_0 where v_1 and v_5 are symmetric vertices about v_0

2. Glue v_2 or v_4 to v_0 where v_2 and v_4 are symmetric vertices about v_0
3. Glue v_3 to v_0
4. Zip up from v_0 so that v_1 and v_5 are glued together

Our goal is to identify all of the rolling belts and isolated gluing trees of the L-shape. Going through our proof, when we reach a gluing tree with a rolling belt, we leave it as an exercise to the reader to determine all different combinatorial types that can be realized on that belt.

Case 1: Due to the symmetry of the right L-shape, gluing v_5 to v_0 is the same as gluing v_1 to v_0 . We simply consider the case of gluing v_1 to v_0 .

Gluing v_1 to v_0 gives this node 2π material, so no other vertices or edges may be glued here. Thus we see that e_1 must be glued to e_5 such that v_2 and v_5 are glued together; this node has π material. We now have a rolling belt that starts at this node and includes e_2 , v_3 , e_3 , v_4 and e_4 because all vertices and nodes have $\leq \pi$ material. This rolling belt accounts for all remaining edges and vertices of the polygon and is thus a valid family of gluings parameterized by a rolling belt. This rolling belt corresponds to the B_1 ring in Figure 7.

Since we have two vertices each with $\frac{\pi}{2}$ material along this big rolling belt, we see that we can alternatively create two smaller rolling belts: a) a rolling belt along e_2 and e_4 or b) a rolling belt along e_3 .

- **Case 1a:** Glue v_3 and v_4 together such that e_3 glues to itself and has a fold point at the midpoint; this node has π material. Starting at this v_3v_4 node, we have a rolling belt that includes e_4 , the v_2v_5 node, and e_2 . This rolling belt accounts for all remaining edges and vertices of the polygon and is then a valid family of gluings parameterized by a rolling belt. This rolling belt corresponds to the B_2 ring in Figure 7.
- **Case 1b:** Glue v_3 and v_4 together such that e_4 glues to the last half of e_2 and the first half of e_2 glues to itself and has a fold point halfway between v_2 and the midpoint of e_2 ; this node has π material. Starting at this node, we have a small rolling belt that includes e_3 . This rolling belt accounts for all remaining edges and vertices of the polygon and is therefore a valid family of gluings parameterized by a rolling belt. This rolling belt corresponds to the B_3 ring in Figure 7.

Notice that if we had instead glued v_5 to v_0 we would have a copy of the B rings for a total of two separate connected components.

Case 2: Due to the symmetry of the right L-shape, gluing v_4 to v_0 is the same as gluing v_2 to v_0 . We simply consider the case of gluing v_2 to v_0 .

Gluing v_2 to v_0 forces v_1 to be a convex-vertex leaf fold. This gluing also causes the node where v_2 and v_0 meet to have 2π material, so no other vertices or edges may be glued to this node. Since no other edges or vertices may be glued here, we see that e_4 must be glued to the first half of e_2 such that v_5 and the midpoint of e_2 are glued together; this node has $\frac{3\pi}{2}$ material. We now have two options. We can either a) continue zipping from this node or b)

put another vertex in this node. We cannot place an edge in this node because that would violate Alexandrov's Theorem.

- **Case 2a** Suppose we continue zipping from this node. Then the rest of e_2 is glued to e_4 so that v_3 and v_4 are glued together; this node has π material. We now have a rolling belt starting at this node that includes e_3 . This accounts for all of the edges and vertices of the polygon and is consequently a valid family of gluings parameterized by a rolling belt. This rolling belt corresponds the A ring in Figure 7.
- **Case 2b** Suppose we put another vertex in the v_5e_2 node. Either v_4 or v_3 are possible candidates since they both have angle $\frac{\pi}{2}$ which, when added to the current total curvature of our node, doesn't violate any part of Alexandrov's Theorem.

If we glue either vertex into the node, then the node has 2π material, so no other vertices or edges may be glued into it. In either case we must zip the edges together until we reach the remaining vertex. This means that the last vertex will be glued to an edge, so this node will have greater than π material. We cannot construct a rolling belt so we must zip up to the final fold point. These two possibilities account for all edges and vertices of the polygon and are hence two valid discreet gluings. In the case of the right L-shape, these two gluing produce the same polyhedron (even though their gluing trees are combinatorially distinct) and correspond to the isolated image Φ in Figure 7.

Again by symmetry we get a copy of A and Φ . Then, together with the B rings we have 4 separate connected components and 2 isolated shapes.

Case 3: Suppose we glue v_3 to v_0 . We see that on either side of this node we have the same symmetric options for gluing the remaining vertices and edges. The following argument will discuss in detail the possible gluings on the v_1 side of the v_0v_3 node and then address the other side.

Gluing v_3 to v_0 causes this node to have 2π material, so by Alexandrov's Theorem, we cannot glue any other vertex or edge to this node. Therefore we must glue the second half of e_2 to e_0 such that v_1 is glued to the midpoint of e_2 ; this node has $\frac{3\pi}{2}$ material. As in Case 2, we now have two options. We can either a) continue zipping from this v_1e_2 node or b) put another vertex in this v_1e_2 node. We cannot place an edge in this node because that would violate Alexandrov's Theorem.

- **Case 3a:** Suppose we continue zipping from this node. Then the rest of e_2 is glued to e_1 so that v_2 is a convex-vertex fold leaf and accounts for all vertices on this half of the original v_0v_3 node.
- **Case 3b:** Suppose we put another vertex in the v_1e_2 node. The vertex available to glue to this node is v_2 , which causes the node to have 2π material. This choice also causes fold points on e_1 and the first half of e_2 and accounts for all vertices on this half of the original v_0v_3 node.

Note that the arguments made for Case a and Case b can be applied to the gluings for other half of the vertices of the L-shape. Then the possible gluings are for the v_1 side of the v_0v_3 node are Case a and Case b and the possible gluings for the v_5 side of the v_0v_3 node are also Case a and Case b, call them Case a' and Case b'. This gives us the combinations of Case a' and Case a, Case a' and Case b, Case b' and Case a, and Case b' and Case b to account for all of the vertices and edges of the L-shape. We see that the combination of Case a' and Case a yields the isolated shape χ , the combination of Case b' and Case b yields the isolated shape Ω , and the combination of Case a' and Case b yields the isolated shape Ψ (note that the combination Case b' and Case a yields an isolated shape that is geometrically the same as Ψ and, as such, is omitted from Figure 7).

Taking these results with the results from Cases 1 and 2 gives six isolated shapes and four separate connected components.

Case 4: Suppose we glue e_0 to e_5 , then v_1 and v_5 are glued together; this node has π material. We now have a rolling belt that starts at this node and includes $e_1, v_2, e_2, v_3, e_3, v_4$ and e_4 because all vertices and nodes have $\leq \pi$ material. This rolling belt corresponds to the C_1 ring in Figure 7.

Since we have three vertices each with $\frac{\pi}{2}$ material along this big rolling belt, we see that we can bring two together, as in Case 1, to create two smaller rolling belts. Whereas in Case 1 there was only one way to choose which two vertices to glue together, in this case there are three (v_2v_3, v_2v_4 , or v_3v_4). Due to the symmetry of the right L-shape, the v_2v_4 and v_3v_4 pairings will clearly generate the same three dimensional structures, where one one side of the two vertex node there is one long edge (e_2 or e_3) and on the other side there is the other long edge (e_3 or e_2) and the two short edges (e_1 and e_4). The third pairing, v_2v_3 , would similarly bring together two $\frac{\pi}{2}$ vertices. In this case we have the two long edges (e_2 and e_3) on one side of the v_2v_3 node and the two short edges (e_1 and e_4) on the other side of the node. However, due to the symmetry of the right L-shape, this situation is equivalent to the case where v_2v_4 or v_3v_4 is the pair of vertices that have been glued together. Thus each of these pairings generate the same three dimensional structures (even though they have structurally distinct gluing trees), so we will only consider the case where we glue v_2 to v_4 . We see that we can create two smaller rolling belts from this big rolling belt: a) a rolling belt along e_2 and e_3 or b) a rolling belt along e_1 and e_4 .

- **Case 4a** Glue v_2 and v_4 together such that e_1 glues to e_4 ; this node has π material. Starting at this node, we have a rolling belt that includes e_2, v_3 , and e_3 . This rolling belt accounts for all remaining edges and vertices of the polygon and is thus a valid family of gluings parameterized by a rolling belt. This rolling belt corresponds to the C_2 ring in Figure 7.
- **Case 4b** Glue v_2 and v_4 together such that e_2 glues to e_3 and v_3 is a convex-vertex leaf; this node has π material. Starting at this node, we have a small rolling belt that includes e_1 and e_4 . This rolling belt accounts for all remaining edges and vertices of the polygon and is thus a valid family of gluings parameterized by a rolling belt. This rolling belt corresponds to the C_3 ring in Figure 7.

Thus we see that the topology of the L-shape has six isolated shapes and five connected components. ■

5 Diagonal Flipping

One of the major difficulties in going from a gluing tree to the final three dimensional realization is determining which vertices or the resulting polyhedron are connected by edges. Current methods for determining edges between n vertices look at all $\binom{n}{2}$ possible edges between them to find the unique combination that results in a convex polytope [10]. This method is inefficient and does not give any strong insight into why certain edges are presenting a crease pattern and others are not.

Issues of determining edges become even more complex when we examine rolling belts. Often, along rolling belts, polyhedral families exhibit the phenomenon of *diagonal flipping*. Diagonal flipping occurs when at a point x_0 on a rolling belt, two triangulated faces become coplanar, forming a flat quadrilateral. Call the vertices of this quadrilateral a , b , c , and d . If before this point x_0 on the belt the edge between the two faces was bd , then as we roll past x_0 the edge flips to ac in order to maintain the convexity of the polyhedron, illustrated in Figure 5. A valid diagonal flip occurs only when the polyhedron maintains convexity as we roll across the point where the diagonal flips.

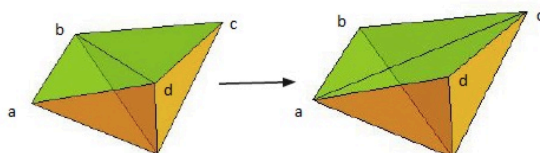


Figure 9: Edge bd flips to edge ac on the flat quadrilateral face.

Three dimensional realizations of the polyhedra along a rolling belt depend on understanding when diagonals flip. Detecting that a diagonal needs to be flipped is not difficult. We check to see if the polyhedron is convex, and if it is not, then we flip the diagonal between the two non-convex faces. On the other hand, determining a point along the rolling belt in which two faces are coplanar is not as simple, especially because as the number of vertices of the polyhedron increases, the number of possible quadrilateral faces also increases.

Diagonal flipping is a concern for us when reconstructing our three dimensional shapes. For an individual crease pattern, diagonal flipping is not a problem. Once we use this singular model to parametrize the entire belt and construct formulas for edge lengths, however, the issue becomes apparent. Diagonal flipping prevents us from extending these formulas along the entire domain of the rolling belt. We must input a different set of edge lengths for each

diagonal flip. A missed diagonal flip, then, results in incorrect edge lengths and thus an incorrect three dimensional realization and a non-convex polyhedron. We investigate each case separately.

Tetrahedra

By definition, diagonal flips cannot occur in tetrahedra; if two faces become coplanar, then the entire polytope folds to a flat quadrilateral. Since each vertex is connected to all other vertices, diagonal flipping is impossible as there are no vertices that are not already connected.

Hexahedra

The hexahedron has the possibility of three degenerate forms: a pentahedron with one quadrilateral face, a tetrahedron, and a flat quadrilateral. This means there is the possibility for diagonal flips as we roll along a rolling belt. In the section *Maximum Volume* we show how diagonal flips in hexahedra affect volume.

Octahedra and Higher

We expect to encounter more complexities as the number of faces of the realized polyhedra increases. We have observed degenerate octahedra with two flat quadrilateral faces, indicating that we will have to consider the possibility of two diagonal flips at once.

6 Edge Relocation

Once we have an understanding of which vertices the edges of the realizable polyhedron lie between, it becomes necessary to look at where these particular edges appear on the crease pattern of the initial polygon. The issue of which edges between vertices of the polyhedron are realized in the crease pattern on the polygon is extremely important for generating three dimensional structures. While there are many geodesic paths connecting two given vertices of a polyhedron, an edge of a polyhedron will be the shortest of these many geodesics between the two vertices. If a physical polyhedron is unfolded, one can determine the location and length of the edges from the physical creases in the paper. This presents a problem when a crease pattern is parameterized by a rolling belt. As we roll along the belt, the the shortest geodesic between two vertices may change location in the crease pattern. This phenomenon, called *edge relocation*, is illustrated in a $\frac{\pi}{3}$ -rhombus in Figure 10.

Edge relocation occurs because as we roll along a rolling belt, the creases (edges on the polyhedron) in the crease pattern parameterized the location on the rolling belt. For any point on the belt, there are infinitely many ways to connect two vertices with a straight line

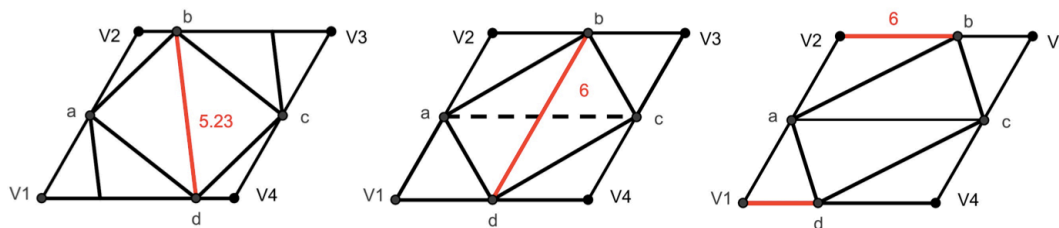


Figure 10: A crease pattern for a parallelogram that is glued into a tetrahedron via an ‘I’-gluing. The red line represents the edge between the tetrahedron vertices b and d . Notice how the edge relocates as we roll past the midway point on the rolling belt.

but at most two shortest distinct creases between the vertices. As the position varies, the length of the creases on the polygon will change.

For the following theorem, we let \mathcal{P} denote the polyhedron folded from polygon P . Let v_i be a vertex of \mathcal{P} and e_i be an edge of \mathcal{P} where $|e_i|$ denotes the length of edge e_i . Define a *potential geodesic* to be the shortest path on \mathcal{P} from v_1 to v_2 . If this potential geodesic is also an edge of \mathcal{P} a *crease* is the projection of this potential geodesic onto the polygon P .

Theorem 4 *Given a polyhedron \mathcal{P} folded from a polygon P with an edge e_1 between polyhedral vertices v_1 and v_2 , there is another potential geodesic edge e_2 between these vertices where $|e_1| = |e_2|$ if and only if \mathcal{P} is flat.*

Proof: We are given that $|e_1| = |e_2|$ are potential edges between v_1 and v_2 . An edge is a straight line in \mathbb{R}^3 between v_1 and v_2 . This means e_1 and e_2 must overlap in \mathbb{R}^3 . Since \mathcal{P} is a convex polytope, then, \mathcal{P} is necessarily flat.

Now suppose that \mathcal{P} is flat. Necessarily, the number of edges of the flat-folded polygon is less than the number of edges of the family of polyhedra of which this flat folding is a degenerate case. Therefore, additional polyhedral edges must cross the surface of the flat-folded polygon. Since this polygon is doubly covered, there exist two potential geodesics, say e_1 and e_2 where $|e_1| = |e_2|$, for each realizable polyhedral edge that crosses the interior of the polygon. ■

Since we define edge relocation as the phenomenon that occurs when the shortest geodesic line between two vertices changes location in the crease pattern, the point of edge relocation occurs when there are two shortest geodesics with the same length. Therefore Theorem 4 is sufficient to say that the point of edge relocation occurs when the polyhedron \mathcal{P} folds flat.

Thus to find all of the edge relocations of a family of polyhedra, we must simply inspect the rolling belt for flat foldings. The problem of finding flat foldings has been well studied and O’Rourke has developed an algorithm for determining flat polyhedra [10].

Corollary 6.1 *Given a polygon, P , with crease pattern C_P , there are at most two shortest distinct creases between a pair of vertices.*

Proof: Suppose not. Then there are n shortest distinct creases between v_1 and v_2 where $n > 2$. An edge is a straight line in \mathbb{R}^3 between v_1 and v_2 . This means e_1, e_2, \dots, e_n must overlap in \mathbb{R}^3 . Then \mathcal{P} is a flat n -covered polygon. But a convex polytope is at most doubly covered. ■

Edge relocation is not a necessarily singular event; in tetrahedra two edges relocate at the same time.

Corollary 6.2 *Given a tetrahedron, \mathcal{T} , folded from polygon P with crease pattern \mathcal{C}_P , edge relocation on \mathcal{C}_P only occurs in pairs.*

Proof: Suppose the edge between v_1 and v_2 of a tetrahedron, \mathcal{T} , relocates. Then, by Lemma 4, \mathcal{T} is flat. Since \mathcal{T} is a tetrahedron, the resulting flat polytope is a doubly-covered quadrilateral. The four edges of the quadrilateral encompass four of the six edges of the tetrahedron. The other two edges must cross the face of the quadrilateral. Since the quadrilateral is doubly covered, there are two potential shortest paths between vertices (one on either side of the polygon). It is given that one of these sets of edges is between v_1 and v_2 . The other must be between a different set of vertices, say v_3 and v_4 . This indicates an edge relocation between these vertices. ■

7 Maximum Volume

Joseph Malkevitch posed the question: What is the maximum volume polyhedron foldable from a given polygon of unit area? In an answer to this question for the unit square, Alexander, Dyson, and O'Rourke found that the maximum volume is achieved by an octahedron with a volume of approximately 0.055849 [4]. This folding is a perimeter halving. Based on this result, O'Rourke and Demaine rephrased Malkevitch's question: Among all planar convex shapes of unit area (smooth shapes or polygons), which folds, via perimeter halving, to the maximum volume (convex) 3D shape [8]? They justify this perimeter halving restriction in light of the fact that smooth shapes fold only by perimeter halving, implying that the largest volume will be the result of folding the square or a smooth shape.

We show that if we were to ask this question for non-convex shapes, we cannot restrict our search to foldings via perimeter halving.

Theorem 5 *In the case of non-convex polygons, perimeter halving does not always yield the maximum volume (convex) three dimensional shape.*

Proof: We prove this theorem by counterexample. In the case of the right angled L-shape, only three distinct convex shapes may be attained via perimeter halving. Two shapes are flat quadrilaterals, and the other is a hexahedron. We use numerical methods to determine that this particular hexahedron has a volume of 0.05000. We use these same methods to

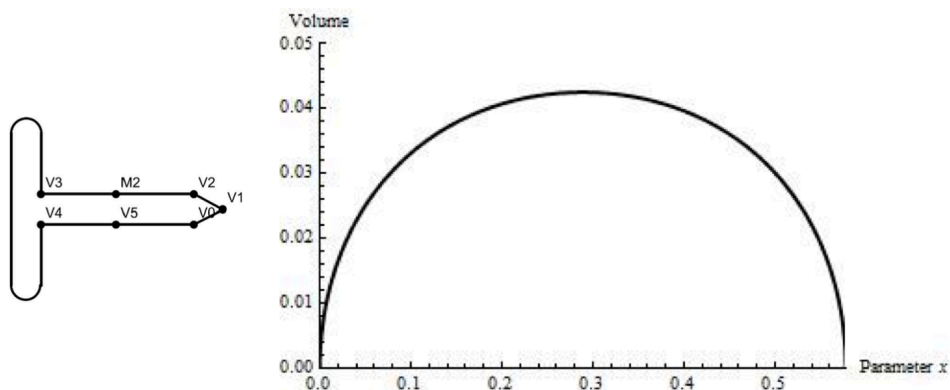


Figure 11: Elliptic volume curve: Change in volume of a tetrahedron formed by folding the right angled L-shape as indicated by the gluing tree on the left. Volume changes as we vary the location on the rolling belt (vertical part of tree).

determine that the maximum volume achieved by any hexahedron folded from the right L-shape has a volume of 0.06415. The structure with this maximal volume is *not* folded via perimeter halving but instead via an edge-to-edge gluing. See Figure 4 for a graphic of this hexahedron. Therefore, perimeter halving does not always yield the maximum volume three dimensional shape for non-convex polygons. ■

Thus, if we are to pose this question for non-convex shapes, we must allow for polyhedra that fold by methods other than perimeter halving.

When dealing with rolling belts, we plot the volume as a function of x , the distance between one of the fold points and a vertex. We used numerical methods to determine the maximum volume. We expected the volume plot to be symmetric about the midpoint of the rolling belt. In some instances, this was the case as in Figure 11. Though we used numerical methods to plot the volume, we were able to fit an elliptic curve to this graph. In this particular case, the elliptic curve could be approximated by the equation $y = 0.02756\sqrt{1 - \left(\frac{x-0.24922}{0.24922}\right)^2}$.

In other instances, however, our volume curves were far from symmetric. See, for example, Figure 12. This depicts the volume of a hexahedral family formed by folding the right angled L-shape in the manner of the gluing tree shown. The maximum volume occurs at approximately $(0.395917, 0.053174)$, which is clearly not halfway along the rolling belt. In fact, this maximum occurs at a point about 34.3% of the length from the vertex, or about 68.6% of the way along the valid interval of the rolling belt.

Plotting the volume becomes increasingly complex as we encounter diagonal flipping. For example, in one of the general gluings of the right angled L-shape, we get a hexahedral family that has two diagonal flips along the valid interval of the rolling belt. This yields three separate sets of parameterized edge lengths, and where they meet we observe a cusp

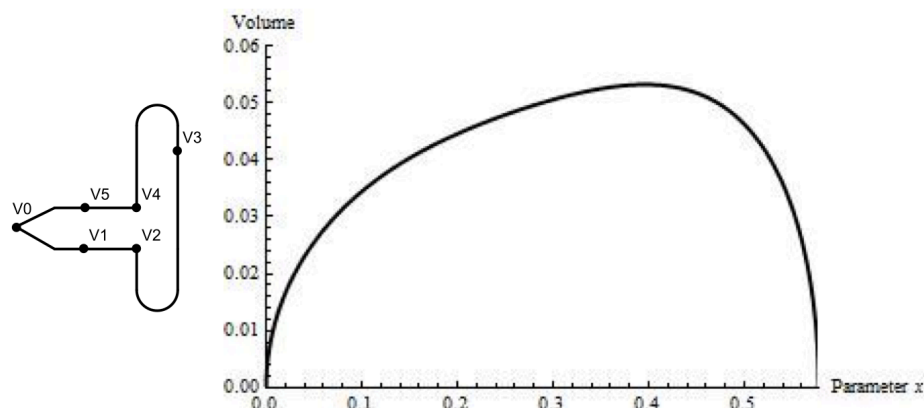


Figure 12: Asymmetric volume curve: Change in volume of a hexahedron formed by folding the right angled L-shape as indicated by the gluing tree on the left. Volume changes as we vary the location on the rolling belt (vertical part of tree).

in the volume plot. Observe Figure 13. The maximum volume hexahedron in this family occurs after the first diagonal flip at approximately $(0.640594, 0.0504879)$. After the second diagonal flip, the volume nears this maximal value but fails to achieve it: the local maximum occurs at approximately $(0.779103, 0.0504717)$.

Another way to approach the question of maximal volume for the family of L-shapes is to look at the change in volume as we vary the angle of the L-shape. We can only do this for structures without rolling belts in order to keep the problem one dimensional. In Figure 14 we study a particular edge-to-edge gluing that yields a hexahedron, and we observe that volume is increasing as a function of the angle α of the L-shape along the interval $[0, \frac{\pi}{2}]$. In other cases, such as that shown in Figure 15, the volume changes in irregular ways. In this case, we graph a general gluing that yields a tetrahedron without a rolling belt and vary α . The graph indicates that the gluing folds flat at an angle of around 0.33 radians.

8 Conclusions and Further Questions

Our research raises several interesting questions regarding diagonal switching, edge relocation, maximum volume, and families of polyhedra realizable from given polygons. We have begun investigations into a few of these questions; we pose some below and share our conjectures:

1. Can we *predict* the exact point at which diagonals will flip?
 - For edge relocation, we were able to determine that this phenomenon occurs at a point of the rolling belt if and only if the polytope folds flat at that point. The

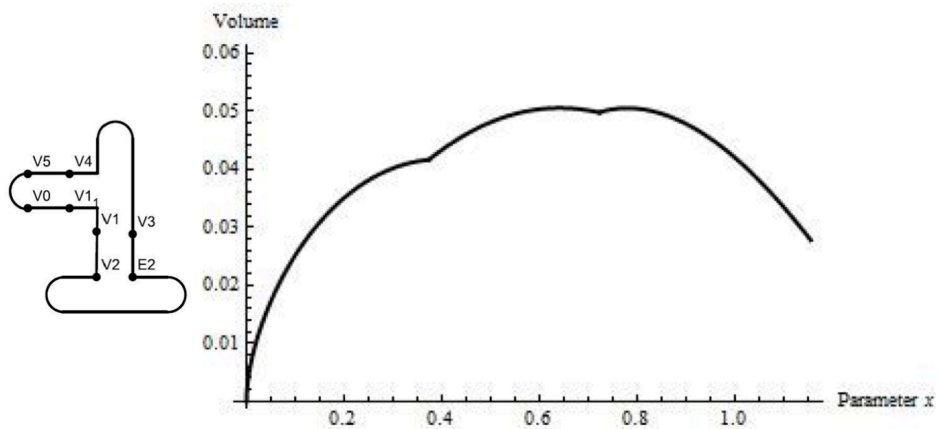


Figure 13: Volume of a polyhedron with diagonal flips: Change in volume of a hexahedron with two diagonal flips. These flips correspond to the cusps at $x \cong .4$ and $x \cong .7$.

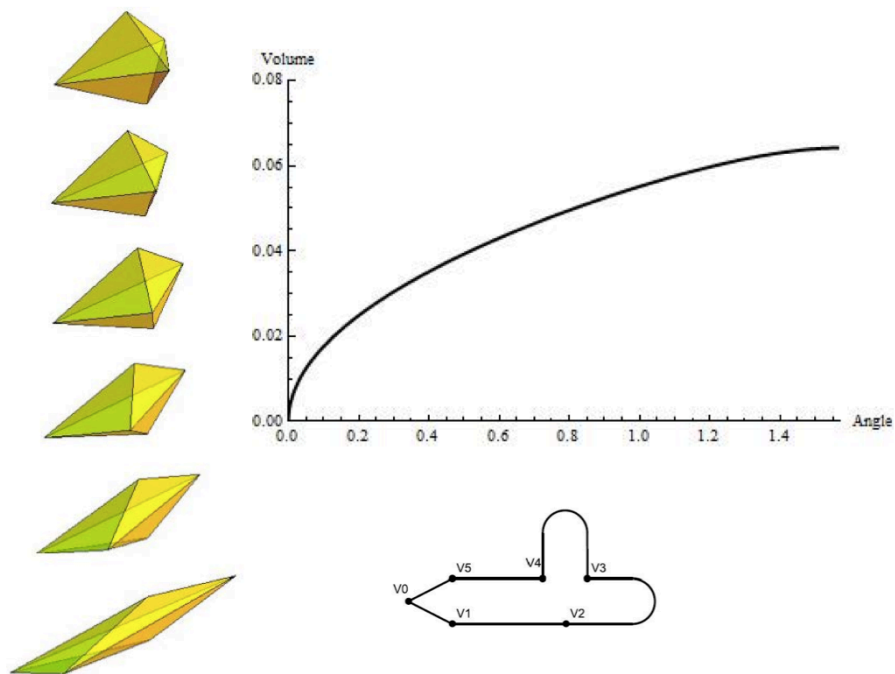


Figure 14: Volume of edge-to-edge foldings with varying angles, α : Change in volume of a hexahedron formed by folding the L-shape as indicated by the gluing tree above as we change the base angle, α . Some 3D realizations are shown for reference.

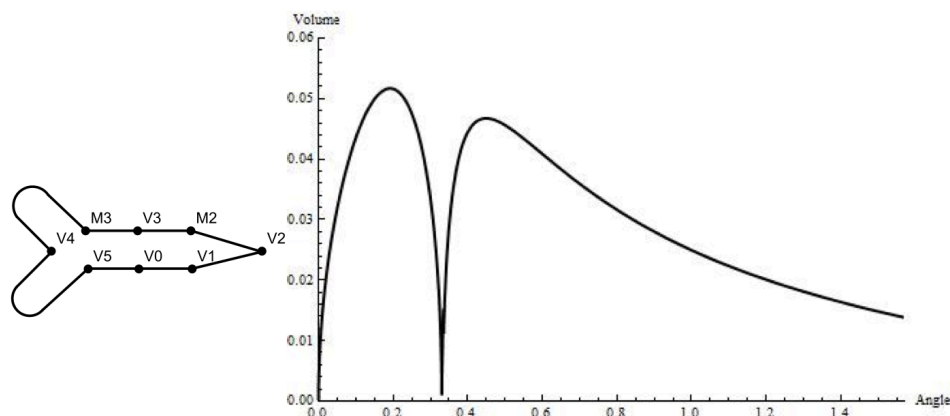


Figure 15: Volume of L-Shapes with varying angle: Change in volume of a tetrahedron formed by folding the right angled L-shape as indicated by the gluing tree as we change the base angle, α . Notice that at $\alpha = 0$ and $\alpha \cong .33$ we have flat foldings.

problem of finding flat polyhedra has been well studied, and thus, we can predict when edge relocation occurs. Determining diagonal flipping, however, is less clear. We know that diagonal flipping occurs at a point if and only if two triangulated faces become coplanar to form one quadrilateral face at that point. Numerical checks on the dihedral angle between two faces may be used to determine when this occurs, but these methods don't provide for an understanding about what is happening to the other edges and faces when a diagonal flips. We would rather use a precise geometric test to predict this occurrence.

2. What is the space of polyhedra foldable from L-shapes with varied edge length?

- We know that polyhedral families ranging from flat polytopes to dodecahedra may be realized by the family of rhombic L-shapes. We conjecture that dodecahedra may be realized by further varying the edge lengths. Further, it is unclear how encompassing these families are; for example, folding L-shapes alone, how much of the space of tetrahedra can we cover?

3. What is the maximum volume polyhedron realizable by an L-shape?

- It seems likely that the maximum volume polyhedron is that with the most vertices. If a dodecahedron *were* realizable from an L-shape, then one of the dodecahedra would likely have the maximum volume.

References

- [1] J. Akiyama, K. Hirata, M. Kobayashi, and G. Nakamura. “Convex developments of a regular tetrahedron. (English summary)” *Comput. Geom.* **34**: 2006, *no. 1*. pp. 2-10. Accessed online at MathSciNet.
- [2] J. Akiyama and G. Nakamura. “Foldings of regular polygons to convex polyhedra.I.Equilateral triangles. (English summary)” *Lecture Notes in Comput. Sci.* **3330**, Springer, Berlin: 2005. pp. 34-43. Accessed online at MathSciNet.
- [3] J. Akiyama and G. Nakamura. “Foldings of regular polygons to convex polyhedra.II.Regular pentagons. (English summary)” *J. Indones. Math. Soc.* **9**: 2003, *no. 2*. pp. 89-99. Accessed online at MathSciNet.
- [4] R. Alexander, H. Dyson, J. O’Rourke. “The Foldings of the Square to Convex Polyhedra.” *Lecture Notes in Comput. Sci.* **2866**, Springer, Berlin: 2003. pp. 38-50. Accessed online at <http://maven.smith.edu/~orourke/Papers/sq.pdf>.
- [5] A. Bobenko, I. Izmistiev. “Alexandrov’s theorem, weighted Delaunay triangulations, and mixed volumes.” *Annulus de l’Institut Fourier*, 58(2):447-505, 2008
- [6] E. Demaine, M. Demaine, J. Itoh, A. Lubiw, C. Nara, J. O’Rourke. “Refold Rigidity of Convex Polyhedra.” *EuroCG 2012*, Assisi, Italy: 2012. pp. 273-276. Accessed online at <http://maven.smith.edu/~orourke/Papers/RefoldRigidEuroCGFull.pdf>.
- [7] E. Demaine, M. Demaine, A. Lubiw, J. O’Rourke. “Enumerating foldings and unfoldings between polygons and polytopes.” *Graphs Combin.* **18**: 2002. pp. 93-104.
- [8] E. Demaine, J. O’Rourke. *Geometric Folding Algorithms: Linkages, Origami, Polyhedra*. New York, NY: Cambridge University Press, 2007.
- [9] A. Lubiw and J. O’Rourke. “When Can a Polygon Fold to a Polytope?” in *Proc AMS Conf.*, Lawerenceville, NJ, Oct 1996.
- [10] J. O’Rourke. “On Flat Polyhedra deriving from Alexandrov’s Theorem.” Jul 2010. Accessed online at <http://arxiv.org/abs/1007.2016>.